

# *Heterorhabditis noenieputensis* n. sp. (Rhabditida: Heterorhabditidae), a new entomopathogenic nematode from South Africa

A.P. Malan<sup>1\*</sup>, R. Knoetze<sup>2</sup> and L. Tiedt<sup>3</sup>

<sup>1</sup>Department of Conservation Ecology and Entomology, Faculty of AgriSciences, Stellenbosch University, Private Bag X1, Matieland 7602, South Africa: <sup>2</sup>Directorate Inspection Services, Department of Agriculture, Forestry and Fisheries, Private Bag X5015, Stellenbosch 7599, South Africa:

<sup>3</sup>Laboratory for Electron Microscopy, North-West University, Potchefstroom Campus, Private Bag X6001, Potchefstroom 2520, South Africa

(Received 24 June 2012; Accepted 29 October 2012)

## Abstract

A new entomopathogenic nematode in the genus *Heterorhabditis* is described from South Africa, from two singular isolates found 1000 km from each other, from beneath a fig tree and in a citrus orchard, respectively. Morphological and molecular studies indicate both isolates to be the same and a new undescribed *Heterorhabditis* species. Comparison of sequences of the internal transcribed spacer (ITS) rDNA and the D2D3 region of the 28S rDNA gene with available sequences of other described species within the genus, indicate the two isolates as a new species. Phylogenetic analysis of the sequence data concerned placed the new species, *H. noenieputensis* n. sp., closest to *H. indica* and *H. gerrardi* in the *indica*-group. The new species, *H. noenieputensis* n. sp., is distinguished from other species in the genus by a combination of several morphological traits of the males and the infective juveniles (IJs). The new species differs from all other species previously described, as regards the body length of the IJs, except for *H. indica* and *H. taysarae*, in which the IJ is smaller. The IJ also differs from that of *H. indica* in the length of the oesophagus, the body diameter, the length of the tail and the E%. In addition, males of *H. noenieputensis* n. sp. differ from their closest relative, *H. indica*, in the position of the excretory pore, SW% and D%; and from *H. gerrardi* in the length of the oesophagus and SW%. The seventh pair of genital papillae of *H. noenieputensis* n. sp. are normally developed, while for *H. indica* they are often branched or swollen at the base, while 8 and 9 are usually absent in both species.

## Introduction

Entomopathogenic nematodes of the genera *Heterorhabditis* and *Steinernema* are of great importance,

as they can be used for the successful control of a wide range of insect pests (Shapiro-Ilan *et al.*, 2002). Despite belonging to two different families, the Heterorhabditidae (Poinar, 1976) and the Steinernematidae (Filipjev, 1934), they have adopted the same biological lifestyle. The free-living stage, called the infective juvenile (IJ) or dauer stage, can be found in soils all over the world. The

---

\*E-mail: apm@sun.ac.za

above-mentioned nematodes are bound in an alliance of mutual benefit with specific symbiotic bacteria, which do not occur freely in nature. The IJ infects the insect host though their natural opening and deposits the symbiotic bacteria, either by means of regurgitation or defecation, in the haemocoel of the insect. In the process of multiplying exponentially, the bacteria kill off the host within a period of 48 h, while the IJ develops into a third-stage feeding larva and into a hermaphrodite in the case of *Heterorhabditis*, or into either a male or female, in the case of *Steinernema*. The nematodes concerned are currently commercially produced and sold as formulated products in Europe and the USA. In South Africa, although some research has already been undertaken into entomopathogenic nematodes, they are not yet commercially available.

In South Africa, only a few surveys have been conducted in which the entomopathogenic nematodes found were identified to species level (Malan *et al.*, 2006, 2011; Hatting *et al.*, 2009). Currently, a total of six species has been reported in South Africa, including the steinernematids, *S. khoisanae* Nguyen, Malan & Gozel, 2006, *S. citrae* Stokwe, Malan, Nguyen & Tiedt, 2011 and *S. yirgalemense* Nguyen, Tesfamariam, Gozel, Gaugler & Adams, 2005. The heterorhabditids include *H. bacteriophora* Poinar, 1976, *H. safricana* Malan, Nguyen, Knoetze & Tiedt, 2008 and *H. zealandica* Poinar, 1990. *Heterorhabditis bacteriophora* was found to be the most frequently occurring species in all surveys that have been conducted in South Africa.

The current number of 17 species for heterorhabditids is relatively low in comparison to the 65 species described for *Steinernema* on a worldwide basis. During 2000–2005, a total of ten new species were described (Nguyen *et al.*, 2006), with, from 2006 to 2011, a total of 28 new species being identified, of which 20 were of *Steinernema* and eight of *Heterorhabditis*. The rapid increase in the rate of description of new species can be ascribed to the use of molecular techniques and to the success obtained in the European and American markets using commercially available species such as *S. feltiae* (Filipjev, 1934) Wouts, Mráček, Gerdin & Bedding, 1982 and *S. carpocapsae* (Weiser, 1955) Wouts, Mráček, Gerdin & Bedding, 1972, and success with new isolates, such as *S. scapterisci* Nguyen & Smart, 1990 and *S. riobrave* Cabanillas, Poinar & Raulston, 1994, against specific target insects. In South Africa surveys have aimed at finding and identifying commercially available species to import for local use.

During a random sampling for indigenous entomopathogenic nematodes, an isolate of *Heterorhabditis* was obtained from a soil sample near the Namibian border in the Northern Cape province of South Africa. A second isolate of the same species were found during a survey of Nelspruit citrus orchards that was undertaken in search of entomopathogenic nematodes with potential to control false codling moth (*Thaumatotibia leucotreta*), which is a key pest of citrus in South Africa (Malan *et al.*, 2011). Morphological and molecular studies showed the two isolates to be the same and to represent a new species of *Heterorhabditis*. The new species is described as *H. noenieputensis* n. sp. [noo.nee.poo.'ten.sis adj.], on the basis of the molecular and morphological evidence presented herein.

## Materials and methods

### *Nematode collection*

*Heterorhabditis noenieputensis* n. sp., isolate SF669 was collected from beneath a fig tree on the farm Springbokvlei, which is situated close to the Namibian border, near the settlement of Noenieput in South Africa. A second isolate (158-C) of the same species was found during a survey for entomopathogenic nematodes in citrus orchards in South Africa in the Nelspruit area (Malan *et al.*, 2011). Larvae of *Galleria mellonella* (L.) (greater wax moth) were used to trap the nematodes from the soil samples (Bedding & Akhurst, 1975). IJs were maintained in the laboratory by recycling through *G. mellonella* larvae every 3 months and by harvesting during the first week of emergence (Dutky *et al.*, 1964). The IJs were stored horizontally in 150 ml filtered water at 14°C in 500-ml culture flasks with vented lids, which were shaken weekly.

### *Morphology*

For taxonomic studies, ten *G. mellonella* were exposed to 200 IJs/insect of the new isolate in each of two 9.0-cm Petri dishes, lined with moistened filter paper and kept in a dark growth chamber at 25°C. The *G. mellonella* larvae died within 2 days after inoculation. First-generation hermaphrodites were obtained 4 days after inoculation and second-generation males and females were collected 6–7 days after death of the insect. Cadavers in one Petri dish were dissected in Ringer's solution, whereas those in the other were transferred to a modified White trap (Kaya & Stock, 1997), with the IJs being harvested within the first week of emergence. For direct observation in order to confirm the morphology or variation of certain structures, the different stages were picked live and killed with gentle heat. After being fixed in TAF (2% triethanolamine, 8% formalin in distilled water) (Courtney *et al.*, 1955), type specimens were processed using the Seinhorst method (Seinhorst, 1959) and mounted in glycerine, using paraffin wax rings to avoid flattening. Measurements were made by means of a compound microscope (Leica DM2000, Leica Microsystems, Wetzlar, Germany) fitted with a digital camera and software Leica Application Suite V3.5.0.

For the morphology of the bursa, males in TAF were transferred to a small drop of lactophenol containing 0.002% acid fuchsin on a glass slide. After 20 min, they were individually transferred to a drop of lactophenol on a glass slide, the tail was removed by using the slanted sharp edge of a syringe needle and the slide covered with a cover slip. By moving the cover slip slightly, using a dissecting needle, the tail was rotated to obtain a ventral view (Nguyen *et al.*, 2004). A total of 20 males were observed by means of the specified method.

Spicules and gubernaculum were prepared by colouring the males for 2 min in a small drop of lactophenol containing 0.002% acid fuchsin on a glass slide. The nematodes were then transferred to a drop of clear lactophenol and the tail cut from the rest of the body using the slanted sharp edge of a syringe needle. The pieces of nematodes severed from the tail were removed and the tails covered with a cover slip,

lightly pressed and moved to free the spicules and gubernaculum from the body. Using this method, a total of 20 males were observed.

For scanning electron microscopy (SEM), hermaphrodites, males, females and IJs were fixed in TAF for a minimum of 3 days, washed three times in 0.05 M cacodylate buffer for 15 min each, and then washed three times in distilled water for 15 min each, after which they were dehydrated in a graded ethanol series (70, 80, 90 and 2 × 100%). The samples were critical point dried with liquid carbon dioxide, mounted on SEM stubs and sputter coated with 20 nm gold/palladium (66/33%). The samples were viewed with an FEI Quanta 200 ESEM (Duren, Germany), operating at 10 kV under high-vacuum mode.

#### Molecular analyses

For DNA extraction, the technique described by Nguyen (2007) was used. One hermaphrodite was placed in 30 ml lysis buffer (500 mM MgCl<sub>2</sub>, 10 mM dithiothreitol (DTT), 4.5% Tween 20, 0.1% gelatine and 3 μl of proteinase K (600 μg/ml)) on the side of a 0.5 μl microcentrifuge tube. The nematode was cut into pieces with the sharp side of a syringe needle and frozen for 1 h at -80°C. The tubes were then incubated in a thermocycler at 65°C for 1 h, followed by incubation at 95°C for 10 min. After centrifugation for 2 min at 12,000 rpm, the supernatant (20 μl) was transferred to a clean microcentrifuge tube and kept at -20°C.

The 18S (5'-TTGATTACGTCCTGCCCTTT-3') and 26S (5'-TTTCACTCGCCGTTACTAAGG-3') primers, suggested by Vrain *et al.* (1992), were used for amplification of the internal transcribed spacer (ITS) region. For the D2D3 region of the 28S rDNA gene, primer D2F (5'-CCTTAGTAACGGCGAGTGAAA-3') and primer 536 (5'-CAGCTATCCTGAGGGAAAC-3') were used (Nguyen *et al.*, 2006). Primers were synthesized by Integrated DNA Technologies Inc. (Coraville, Iowa, USA). Nguyen's (2007) technique was followed for polymerase chain reaction (PCR) amplification.

Post-PCR purification was undertaken using the NucleoFast Purification System (Macherey Nagel, Waltham, Massachusetts, USA). Sequencing was performed with the BigDye Terminator V1.3 sequencing kit (Applied Biosystems), followed by electrophoresis on the 3730 × 1 DNA Analyser (Applied Biosystems, Foster City, California, USA) at the DNA Sequencing Unit (Central Analytical Facilities, Stellenbosch University). Sequence assembly and editing were performed using the software CLC Main Workbench (ver. 6.6.2; <http://www.clcbio/products/clc-main-workbench/>).

The GenBank numbers of the ITS and D2D3 region of the 28S rDNA gene sequences used in the phylogenetic analyses are indicated in the phylogenetic trees. Sequences were aligned using ClustalX 1.83 with default options (Thompson *et al.*, 1997). Distance analysis of the closest taxa (number of base differences per sequence) was conducted in MEGA5 (Tamura *et al.*, 2011).

The evolutionary history of the ITS and the D2D3 region was inferred using the neighbour-joining method (Saitou & Nei, 1987). A bootstrap consensus tree was inferred from 1000 replicates. The evolutionary distances were computed using the Jukes-Cantor

method (Jukes & Cantor, 1969). All ambiguous positions were removed for each sequence pair. Evolutionary analyses were conducted in MEGA5 (Tamura *et al.*, 2011).

## Results and discussion

#### Description of *Heterorhabditis noenieputensis* n. sp.

The specific epithet is derived from the name of the settlement Noenieput, which is situated close to where the species was found on the farm Springbokvlei. Figures 1–4 illustrate the description, and morphometrics of adult and third-stage juvenile stages are presented in table 1.

#### Morphology

**Male:** Posterior third of the body slightly curved ventrally in a J-shape when killed with heat. Cuticle smooth, but showing light striation on SEM. Head truncate, sometimes slightly swollen. Six labial papillae, cephalic papillae not observed. Amphidial openings were not conspicuous. Mouth opening funnel-shaped. Stoma with sclerotized rod or barrel-shaped cheilorhabdions; other rhabdions indistinguishable, forming a funnel-shaped structure posterior to cheilorhabdions. Oesophagus with

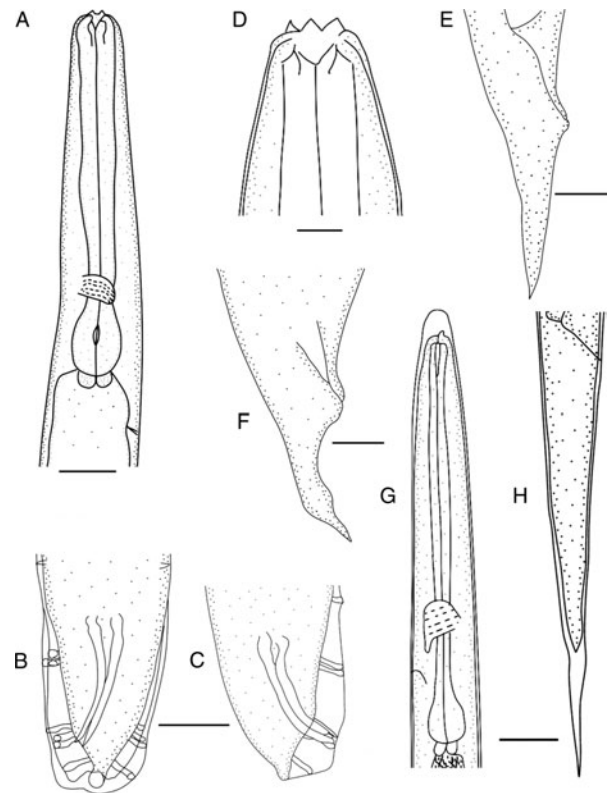


Fig. 1. *Heterorhabditis noenieputensis* n. sp. line drawings. (A–C) Male: (A) anterior region; (B, C) ventral and lateral view of tail showing spicules and genital papillae. (D–F) Hermaphrodite: (D) head region; (E, F) variation in the tail. (G, H) Third-stage infective juvenile: (G) anterior region; (H) tail region. Scale bars: A–C, E–H = 20 μm; D = 10 μm.

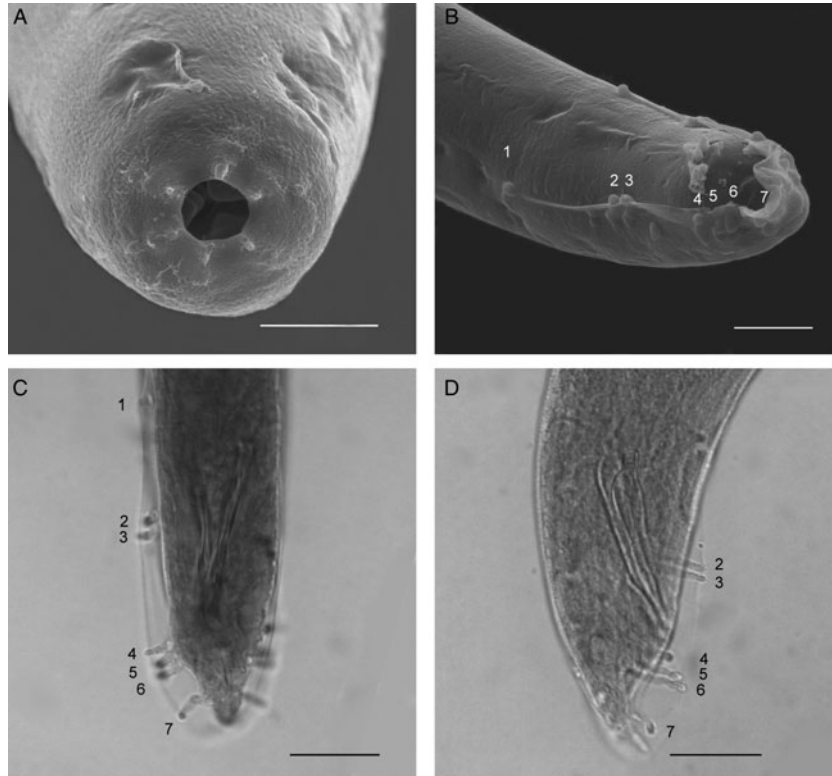


Fig. 2. *Heterorhabditis noenieputensis* n. sp. (A) Head region of second-generation male, showing mouth opening and six labial papillae. (B) Posterior region, showing anal aperture and bursa papillae. (C) Ventral view of male tail, showing arrangement of bursal papillae. (D) Lateral view of male tail, showing the arrangement of papillae. Scale bars: A = 5  $\mu\text{m}$ ; B = 10  $\mu\text{m}$ ; C, D = 20  $\mu\text{m}$ .

cylindrical corpus, metacarpus slightly enlarged. The isthmus distinct. The basal bulb pyriform with lumen of the oesophagus with sclerotized valve. Nerve ring surrounding the isthmus just anterior to the basal bulb. Excretory pore well posterior to the basal bulb. Cardia present, protruding into intestine. Excretory pore usually posterior to basal bulb. Testis monarchic and reflexed anteriorly. Vas deferens well developed. Spicules paired without a rostrum, lamina of spicules slightly curved ventrally. Gubernaculum slightly curved ventrally, about half the size of the spicules. Tail conoid slightly curved ventrally, with peloderan bursa. Seven to eight pairs of bursal papillae (bursal rays) present on bursa. From anterior to posterior, pair 1 well anterior from cloaca, with papilla tips extending to bursal rim; pairs two and three in a group anterior to the cloaca, also extending beyond the bursal rim. Pairs 4, 5 and 6 forming a group posterior to the cloaca, extending beyond the bursal rim, with pair 4 aimed outwards laterally. Number of genital papillae from pairs 1–7 (from anterior end) is unchanged and typical for *Heterorhabditis* species (Nguyen, 2007). Observation of papillae of the terminal group of 10 bursas gave the following results: eight with both pairs 8 and the 9 absent; three with pair 8 present and one with one papillae of pair 8 missing.

*Hermaphrodite*: Body curved posteriorly in an open to closed C-shape after killing with gentle heat, robust,

always with many eggs in young females and many eggs and juveniles in mature females. Cuticle smooth under light microscope, but finely annulated under SEM. Head region tapering gently anteriorly, six distinct outwardly curved protruding lips, each bearing a prominent labial papilla. *En face* view, mouth hexagonal in shape, with two pore-like amphidial apertures. An outer ring of ten cephalic papillae is observable, with two lateral, four dorso-lateral and four ventro-lateral. Stoma with refractile cheilorhabdions, appearing as a circle below the lips. Posterior part of stoma funnel-shaped. Oesophagus with cylindrical corpus. Nerve ring in vicinity of narrowed isthmus, between corpus and basal bulb. Basal bulb prominent with inconspicuous valve, lumen of oesophagus in basal bulb well sclerotized. Opening of excretory pore located posterior to end of oesophagus. Cardia present and well developed. Gonads didelphic, amphidelphic. Vulva in form of a transverse slit, located anterior to midbody on a slightly protruding area. In ventral view, vulva elliptical, encircled by arch-shaped annules anteriorly and posteriorly. Vagina short. Tail longer than anal body diameter, in some cases forming a thickening before ending in a pointed terminus. Slight post-anal swelling present. Phasmid inconspicuous.

*Amphimictic female*: Similar to hermaphroditic female, but smaller. Vulva non-protruberant, usually covered with exudates or copulation plug after mating. Post-anal

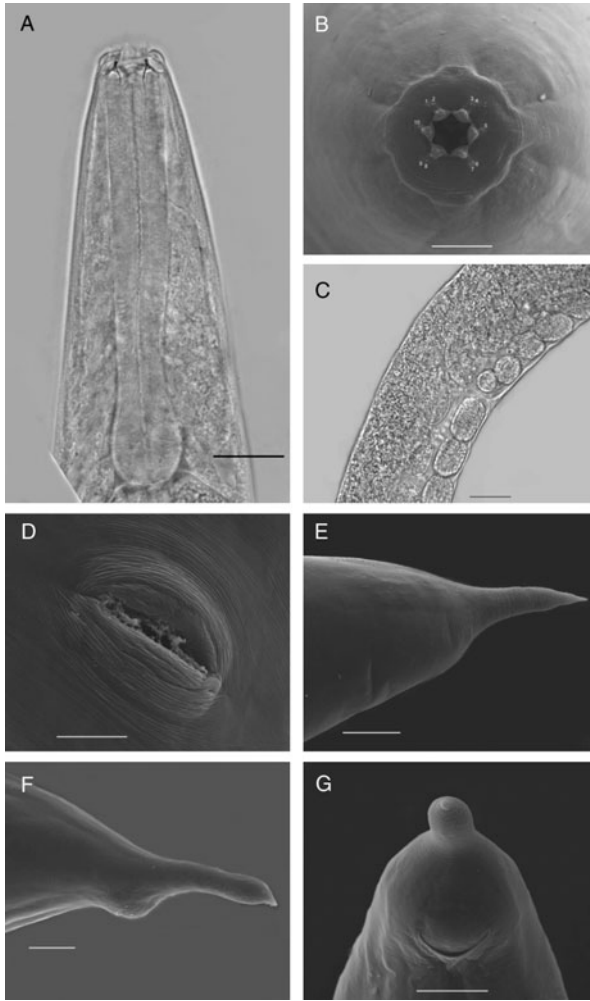


Fig. 3. *Heterorhabditis noenieputensis* n. sp. (A) Oesophagus of the hermaphroditic female. (B) *En face* view of the hermaphroditic female, showing six prominent outward protruding lips, each bearing an observable prominent labial papilla and an outer ring of ten cephalic papillae. (C) Vulva of amphimictic female covered with exudates or copulation plug. (D) Vulva with elliptical pattern. (E, F, G) Variation in the hermaphroditic female tail. Scale bars: B, D = 10  $\mu$ m; A, E, F, G = 20  $\mu$ m; C = 50  $\mu$ m.

swelling less pronounced. Tail does not form a bulbous variation, but is always conoid with a pointed terminus.

*Infective juvenile (IJ)*: Body long and slender. Sheath (second-stage cuticle) enclosed in the second-stage juvenile cuticle. The sheath is notably loose and projecting well in front of the head, or can be attached to the head and folded backwards. Ensheathed larvae with lateral field showing two ridges and exsheathed third-stage IJ with fine annulations. Labial region with a conspicuous visual dorsal tooth and amphidial apertures. Oesophagus narrow, isthmus long and narrow, basal bulb pyriform with small valve. Excretory pore in anterior to the basal bulb. Tail long, pointed. Amphidial aperture prominent, pore-like. Excretory duct not pronounced or cuticularized. Oesophagus typical of genus. Lateral field at midbody.

*Type host and material*

The natural host of *H. noenieputensis* n. sp. is unknown, as the nematode was trapped by baiting a single soil sample with *G. mellonella*. *Heterorhabditis noenieputensis* n. sp., isolate SF669 was collected from a single soil sample that was obtained from beneath a fig tree on the farm Springbokvlei, which is situated close to the Namibian border, near the settlement of Noenieput (27°27'.149S/20°05'.716E) in South Africa. A second isolate (158-C) of the same species was found in a single soil sample during a survey for entomopathogenic nematodes from citrus orchards in the Nelspruit area of South Africa (25°28'.639S/31°02'.549E), which covered approximately 1130 km east to west (Malan *et al.*, 2011).

Holotype male (mounted) and 20 paratypes each of hermaphrodites, females, males, and many IJs in TAF, isolated from the haemocoel of *G. mellonella*, are deposited in the United States Department of Agriculture,

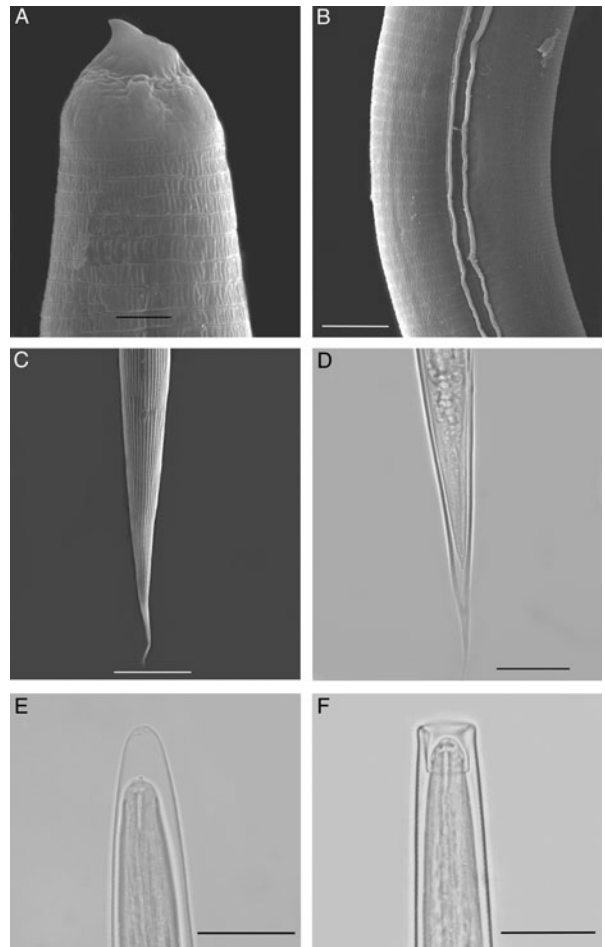


Fig. 4. *Heterorhabditis noenieputensis* n. sp. (A) Anterior of exsheathed IJ, showing the amphidial aperture and the dorsal tooth. (B) Longitudinal ridges of exsheathed IJ. (C) Tail of ensheathed IJ, showing lateral ridges. (D) Ensheathed IJ, showing the position of the anus. (E, F) Head region of the IJ, showing the sheath variation. Scale bars: A = 2  $\mu$ m; B = 5  $\mu$ m; C = 20  $\mu$ m; D–F = 20  $\mu$ m.

Table 1. Morphometrics of different stages of *Heterorhabditis noenieputensis* (SF669) n. sp. All measurements in  $\mu\text{m}$  and in the form: mean  $\pm$  SD (range).

Character	Male			Hermaphrodite	Female	Infective	
	Holotype	Paratypes		1st Generation	2nd Generation	juvenile	
		SF669	SF669	SF158-C	SF669	SF669	SF669
<i>n</i>		20	20	20	20	25	25
Body length (L)	644	649 $\pm$ 72 (530–775)	653 $\pm$ 59 (542–758)	4323 $\pm$ 555 (2987–5498)	1409 $\pm$ 151 (1075–1697)	536 $\pm$ 21 (484–578)	528 $\pm$ 21 (484–563)
a = L/MBD	17	16 $\pm$ 1.2 (14–18)	18 $\pm$ 2.2 (13–23)	18 $\pm$ 2.3 (14–23)	15 $\pm$ 1.0 (13–17)	24 $\pm$ 1.4 (21–27)	25 $\pm$ 0.1 (24–28)
b = L/ES	6.8	6.8 $\pm$ 0.6 (5.6–7.9)	7.2 $\pm$ 0.6 (5.9–8.4)	22 $\pm$ 2.2 (18–28)	12 $\pm$ 1.3 (9–14)	4.9 $\pm$ 0.2 (4.3–5.2)	5.3 $\pm$ 1.0 (4.9–8.1)
c = L/T	24	26 $\pm$ 4 (21–33)	26 $\pm$ 4 (18–32)	47 $\pm$ 6.3 (37–58)	21 $\pm$ 1.9 (17–24)	6.2 $\pm$ 0.3 (5.5–6.8)	5.9 $\pm$ 0.6 (5.0–8.1)
c' = T/ABD	1.44	1.3 $\pm$ 0.3 (1.05–1.65)	0.9 $\pm$ 0.6 (0.2–1.6)	2.1 $\pm$ 0.4 (1.7–3.4)	2.7 $\pm$ 0.2 (2.3–3.1)	3.8 $\pm$ 0.3 (3.4–4.3)	6.6 $\pm$ 0.5 (4.9–7.1)
V%	–	–	–	43 $\pm$ 6.4 (39–47)	47 $\pm$ 2.6 (40–53)	–	–
Max. body diameter (MBD)	39	41 $\pm$ 3 (34–46)	38 $\pm$ 3.3 (33–46)	239 $\pm$ 37 (168–289)	96 $\pm$ 13 (76–129)	23 $\pm$ 1 (21–25)	21 $\pm$ 1 (19–23)
Stoma length	7.3	7.1 $\pm$ 1.4 (4.8–9.2)	6.6 $\pm$ 1.2 (4.9–8.6)	14.7 $\pm$ 1.9 (12.3–18.7)	9.1 $\pm$ 1.2 (6.3–10.4)	–	–
Stoma diameter	4.9	4.7 $\pm$ 0.5 (4.1–5.5)	4.5 $\pm$ 0.5 (4.2–5.7)	11.2 $\pm$ 1.1 (9.2–13.4)	8.3 $\pm$ 1.1 (6.3–10.2)	–	–
EP	102	86 $\pm$ 7.1 (75–102)	102 $\pm$ 8 (84–114)	183 $\pm$ 17 (152–209)	113 $\pm$ 7 (102–125)	97 $\pm$ 3.4 (88–105)	91 $\pm$ 8.4 (79–113)
NR	67	67 $\pm$ 3 (64–75)	71 $\pm$ 4 (63–78)	133 $\pm$ 12 (112–152)	84 $\pm$ 4.7 (73–90)	81 $\pm$ 6.3 (69–96)	74 $\pm$ 5.9 (70–87)
ES	94	95 $\pm$ 5.2 (88–106)	92 $\pm$ 3 (86–98)	199 $\pm$ 13 (166–220)	123 $\pm$ 5 (115–132)	106 $\pm$ 9.1 (79–115)	103 $\pm$ 3.1 (99–108)
Hemizonion	–	–	–	–	–	92 $\pm$ 4.2 (82–102)	83 $\pm$ 3.8 (76–93)
Testis reflexion	97	82 $\pm$ 11 (67–104)	73 $\pm$ 12 (50–100)	–	–	–	–
Tail length (T)	27	25 $\pm$ 2.4 (21–32)	26 $\pm$ 2 (23–30)	94 $\pm$ 12 (79–120)	69 $\pm$ 4 (63–75)	86 $\pm$ 3 (78–95)	86 $\pm$ 6 (80–92)
Tail length without sheath	–	–	–	–	–	60 $\pm$ 2.8 (55–66)	66 $\pm$ 4.97 (56–76)
Anal body diameter (ABD)	19	19 $\pm$ 1.9 (15–22)	19 $\pm$ 1 (17–21)	45 $\pm$ 7.7 (26–56)	26 $\pm$ 3 (22–32)	14 $\pm$ 1.0 (12–16)	13 $\pm$ 1.0 (12–13)
Spicule length (SP)	47	43 $\pm$ 3.5 (37–49)	42 $\pm$ 3 (35–48)	–	–	–	–
Spicule width	5.03	5.18 $\pm$ 0.63 (3.92–6.55)	–	–	–	–	–
Gubernaculum length (GU)	21	20 $\pm$ 2 (17–24)	19 $\pm$ 2 (15–24)	–	–	–	–
D% = EP/ES $\times$ 100	108	90 $\pm$ 6.2 (81–108)	110 $\pm$ 9 (88–120)	93 $\pm$ 8.7 (77–112)	92 $\pm$ 6 (83–104)	89 $\pm$ 3 (81–95)	92 $\pm$ 8 (83–111)
E% = EP/T $\times$ 100	372	350 $\pm$ 38 (270–430)	391 $\pm$ 37 (303–464)	198 $\pm$ 22 (158–230)	166 $\pm$ 16 (143–192)	113 $\pm$ 6.1 (99–125)	107 $\pm$ 9.8 (85–124)
SW% = SP/ABD $\times$ 100	247	231 $\pm$ 24 (202–301)	221 $\pm$ 20 (185–271)	–	–	–	–
GS% = GU/SP $\times$ 100	45	47 $\pm$ 3.9 (38–56)	47 $\pm$ 5 (38–54)	–	–	–	–

V% = distance from anterior end to vulva/body length; EP, distance from anterior end to excretory pore; NR, distance from anterior end to nerve ring; ES, distance from anterior end to end of oesophagus.

Nematode Collection (USDANC), Beltsville, Maryland, USA. In addition, 20 paratypes each of hermaphrodites, males, females and many IJs in TAF are deposited in the National Collection of Nematodes, Biosystematics Division, Plant Protection Research Institute, Agricultural Research Council, Pretoria, South Africa. Slides of one male and one

female of the second generation, and of several IJs are deposited in the California Collection of Nematodes, University of California-Davis Nematode Collection, Davis, California, USA. Several slides of hermaphrodites, males, females and all stages in TAF are maintained in the Department of Entomology at Stellenbosch University.

Table 2. Pairwise distances of ITS and D2D3 regions between taxa.

Species	1	2	3	4	5	6	7	8	9	10	11	12	13	14	15	16	17	18	
ITS region																			
1	<i>H. noenieputensis</i> n. sp.	–																	
2	<i>H. amazonensis</i>	77	–																
3	<i>H. atacamensis</i>	146	155	–															
4	<i>H. bacteriophora</i>	149	157	113	–														
5	<i>H. baujardi</i>	79	8	155	152	–													
6	<i>H. downesi</i>	157	162	25	121	159	–												
7	<i>H. floridensis</i>	81	11	159	159	11	166	–											
8	<i>H. georgiana</i>	150	160	118	15	155	125	162	–										
9	<i>H. gerrardi</i>	9	75	142	147	77	153	81	148	–									
10	<i>H. indica</i>	10	76	145	148	78	156	82	149	3	–								
11	<i>H. marelatus</i>	155	160	20	115	159	34	164	121	151	154								
12	<i>H. megidis</i>	164	170	44	131	168	33	173	137	160	163	51	–						
13	<i>H. mexicana</i>	84	14	160	164	17	166	11	167	82	83	165	172						
14	<i>H. safricana</i>	153	162	11	119	161	29	166	123	149	152	23	47	167	–				
15	<i>H. sonorensis</i>	84	13	159	165	17	165	12	166	82	83	166	171	8	166	–			
16	<i>H. taysearae</i>	85	14	158	164	18	164	13	165	83	84	165	170	9	165	1	–		
17	<i>H. zealandica</i>	178	181	67	145	180	71	184	150	174	177	69	86	184	72	186	185	–	
18	<i>C. elegans</i>	316	312	297	308	313	303	312	309	314	315	295	299	314	298	311	311	310	–
D2D3 regions																			
1	<i>H. noenieputensis</i> n. sp.																		
2	<i>H. amazonensis</i>	19	–																
3	<i>H. atacamensis</i>	36	32	–															
4	<i>H. bacteriophora</i>	39	33	24	–														
5	<i>H. floridensis</i>	21	4	35	34	–													
6	<i>H. georgiana</i>	40	36	25	3	37	–												
7	<i>H. indica</i>	1	20	36	39	22	40	–											
8	<i>H. marelatus</i>	37	35	3	27	38	28	37	–										
9	<i>H. megidis</i>	42	40	10	33	43	34	42	11	–									
10	<i>H. mexicana</i>	19	4	31	32	4	35	20	34	39	–								
11	<i>H. safricana</i>	34	36	5	29	39	30	34	6	13	35	–							
12	<i>H. zealandica</i>	41	37	9	29	40	30	41	10	11	36	12	–						
13	<i>C. elegans</i>	133	136	132	136	139	135	133	134	129	136	132	130	–					

Heterorhabdus noenieputensis n. sp.

### Molecular characterization

The ITS rDNA regions, flanked by primers 18S and 26S, of *H. noenieputensis* n. sp. (JN620538) are characterized by the sequence length of 1032 base pairs (ITS1 = 371, ITS2 = 216). Pairwise distances between closely related species (table 2) show that *H. noenieputensis* n. sp. differs from *H. gerrardi* and *H. indica* by 9 and 10 base pairs, respectively in the ITS regions. The new species is most divergent from *H. zealandica*, from which it differs in 178 aligned positions (table 2).

The D2D3 region of the 28S rDNA gene (JX624110) of *H. noenieputensis* n. sp., flanked by the primers D2F and 536, is characterized by 898 base pairs. It differs from both *H. amazonensis* and *H. indica* in only one base pair and differs the most from *H. georgiana* and *H. bacteriophora* in eight base pairs. The nucleotide usage of the D2D3 region of the 28S rDNA gene is A = 0.25 230; C = 0.29 130; G = 0.19 400; T = 0.25 860. Pairwise distances also show that the closest related species is *H. indica*, with only one base pair difference, and the most divergent from *H. megidis*, from which it differs in 42 aligned positions (table 2). *Heterorhabditis noenieputensis* n. sp. also has the six unique base pairs (table 3), that are present in only in members of the *indica*-group (Nguyen *et al.*, 2008).

Phylogenetic relationships of *H. noenieputensis* n. sp. with closely related species inferred from ITS rRNA sequences by using the neighbour-joining and maximum parsimony methods give very similar trees (fig. 5). The bootstrap consensus tree included two weakly supported monophyletic groups. In the first, the *indica*-group, *H. noenieputensis* n. sp., *H. gerrardi* and *H. indica* comprise a monophyletic group with adequate bootstrap support (89%). The other monophyletic sister group is formed by *H. amazonensis*, *H. baujardi*, *H. floridensis*, *H. mexicana*, *H. taysearae* and *H. sonorensis*, with weaker bootstrap support (85%). The second group, the *megidis*-group, was formed by eight other species. Phylogenetic relationships of *H. noenieputensis* n. sp., with closely related species inferred from the D2D3 region of the 28S rDNA gene sequences by using the neighbour-joining method based on the Jukes–Cantor model, yielded a bootstrap consensus tree with similar topology, but with better bootstrap support for the different groups (fig. 6).

We conclude that the morphological and molecular characteristics that we found are sufficient to regard *H. noenieputensis* n. sp. as a new species.

### Diagnosis and relationships with other species

*Heterorhabditis noenieputensis* n. sp. can be distinguished from other *Heterorhabditis* species by a combination of morphological and morphometric traits (tables 4, 5, figs 1–4). Males of the new species have the typical arrangement of genital papillae for the first seven pairs from anterior to posterior. Pairs eight can be present in 30% of the cases, while pair nine is always absent. In 10% of cases, only one pair of eight is visible on the one side. The males of *H. indica* differ, in that the seventh pair of genital papillae is often branched or swollen at the base, is variable in form and may or may not reach the bursal rim, while the eighth and ninth pairs of papillae are also usually absent. In the males of *H. gerrardi* the terminal pairs seven, eight and nine are usually present. In addition, males of *H. noenieputensis* n. sp. differ from their closest relative, *H. indica*, in the position of the excretory pore (86  $\mu$ m versus 123  $\mu$ m), SW% (231 versus 187) and D% (90 versus 121), and from *H. gerrardi* in the length of the oesophagus (95  $\mu$ m versus 103  $\mu$ m) and SW% (231 versus 183) (table 4).

The hermaphrodite of *H. noenieputensis* n. sp. differs from that of *H. gerrardi* in the outwardly protruding lips, a characteristic it shares with *H. indica*. The tails of the new species differ from all other species in that the tail of the hermaphrodite forms a thickening before ending in a pointed terminus.

The third-stage IJ of *H. noenieputensis* n. sp. differs in body length (536  $\mu$ m (484–578)) from all other *Heterorhabditis* spp., except for *H. taysearae* and *H. indica* which have body lengths of 418  $\mu$ m (332–499) and 528  $\mu$ m (478–573), respectively. The body length of the IJ of *H. noenieputensis* n. sp. shows an overlap with that of *H. indica*, but also differs from *H. indica* in the length of the oesophagus (106  $\mu$ m versus 117  $\mu$ m), the body diameter (23  $\mu$ m versus 20  $\mu$ m), the length of the tail (86  $\mu$ m versus 101  $\mu$ m) and the E% (113 versus 94) (table 5). Curiously, the third-stage IJ of both isolates of *H. noenieputensis*

Table 3. Selected portion of the alignment of D2D3 expansion regions of *Heterorhabditis* showing an indel fragment with six unique bold-faced base pairs (687–692) in sequences of species in the *indica*-group.

Species	Sequence
	651 687 692 700
<i>H. bacteriophora</i>	AAGGCCGGTT--AACC GGTTGACATGGGATCCGC-----TCTTCGGA
<i>H. marelatus</i>	AAGACTAGTT--AACTAGTTGACATGGGATCCGC-----TCTTCGGA
<i>H. zealandica</i>	AAGACTAGTT--AACTAGTTGACATGGGATCCGC-----TCTTCGGA
<b><i>H. noenieputensis</i> n.sp.</b>	AAGACCGGTT--AACC GGTTGACATGGGATCCGACT <b>GA</b> ACTTCTTCG-A
<i>H. mexicana</i>	AAGGCCGGTT--AACC GGTTGACATGGGATCCGAT <b>GA</b> ACTTCTTCG-A
<i>H. amazonensis</i>	AAGGCCGGTT--AACC GGTTGACATGGGATCCGAAT <b>GA</b> ACTTCTTCGAA
<i>H. floridensis</i>	AAGGCCGGTT--AACC GGTTGACATGGGATCCG <b>TG</b> ACTTCTTCGAA
<i>H. indica</i>	AAGACCGGTT--AACC GGTTGACATGGGATCCGACT <b>GA</b> ACTTCTTCGAA
<i>H. atacamensis</i>	AAGACTAGTT--AACTAGTTGACATGGGATCCGC-----TCTTCGGA
<i>H. megidis</i>	AAGACTAGTT--AACTAGTTGACATGGGATCCGC-----TCTTCGGA
<i>C. elegans</i>	AAGGTCAGTCTCGAATTGGCCGACGTGGGATCTGTG----TTCTTCGGA



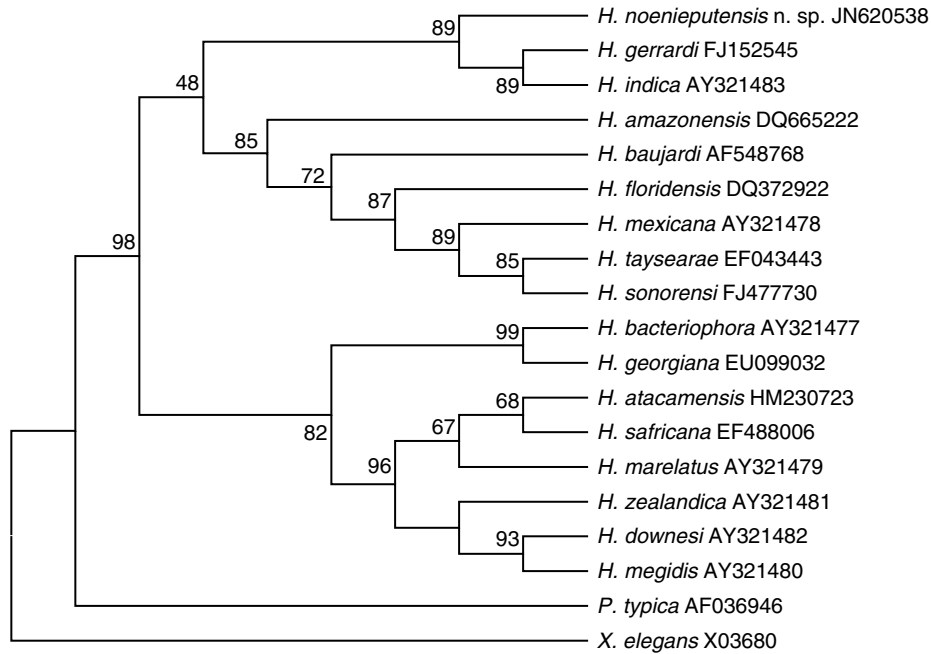


Fig. 5. Phylogenetic relationship of 17 species of *Heterorhabditis* based on analysis of the ITS rDNA region using the neighbour-joining method. The bootstrap consensus tree inferred from 1000 replicates is taken to represent the evolutionary history of the taxa analysed. The percentage of replicate trees in which the associated taxa clustered together in the bootstrap test is shown next to the branches. The evolutionary distances were computed using the Jukes–Cantor method.

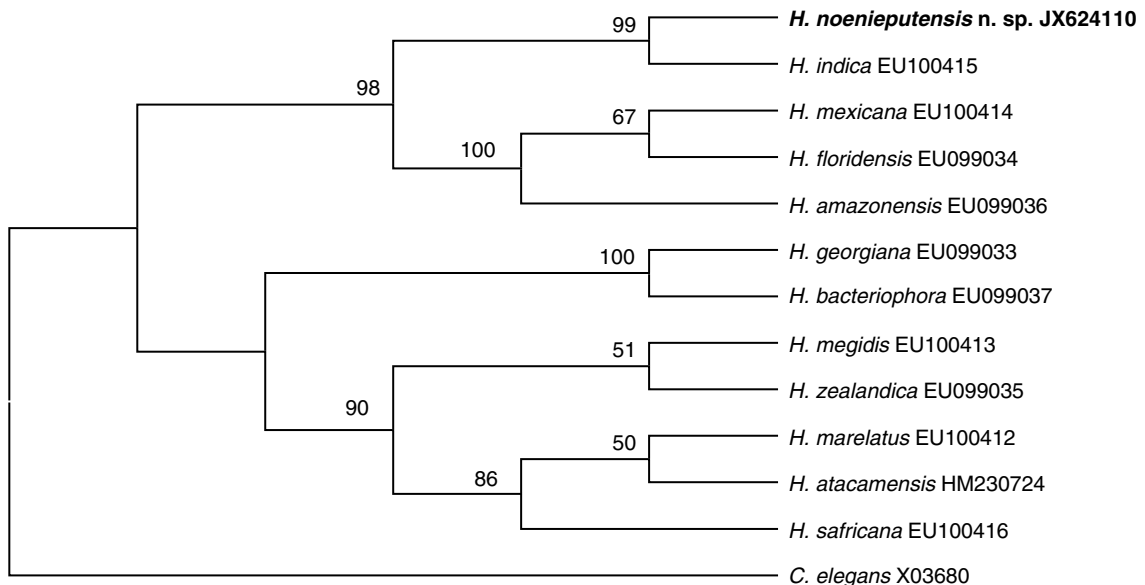


Fig. 6. Phylogenetic relationship of *Heterorhabditis noenieputensis* n. sp. based on the analysis of the D2D3 region of the 28S rDNA gene, using the neighbour-joining method. The bootstrap consensus tree inferred from 1000 replicates is taken to represent the evolutionary history of the taxa analysed. The percentage of replicate trees in which the associated taxa clustered together in the bootstrap test is shown next to the branches. The evolutionary distances were computed using the Jukes–Cantor method.

Table 4. Comparative morphometrics of male of *Heterorhabditis noenieputensis* n. sp. (in bold) and other related species. All measurements in  $\mu\text{m}$  and in the form: mean (range) or mean  $\pm$  SD (range).

Character	TAY Shamseldean <i>et al.</i> (1996)	IND Poinar <i>et al.</i> (1992)	NOE n. sp. <b>SF669</b>	BAU Phan <i>et al.</i> (2003)	SOR <sup>a</sup> Stock <i>et al.</i> (2009)	FLO Nguyen <i>et al.</i> (2006)	MEX Nguyen <i>et al.</i> (2004)	AMA Andaló <i>et al.</i> (2006)	GEO Nguyen <i>et al.</i> (2008)	SAF Malan <i>et al.</i> (2008)	GER Plichta <i>et al.</i> (2009)	DOW <sup>b</sup> Stock <i>et al.</i> (2002)
<i>n</i>	20	12	<b>20</b>	14	20	20	20	20	20	20	20	19
Body length (L)	703 $\pm$ 23 (648–736)	721 $\pm$ 64 (573–788)	<b>649 <math>\pm</math> 72 (530–775)</b>	889 $\pm$ 45 (818–970)	725 $\pm$ 31 (500–750)	862 $\pm$ 44 (785–924)	686 $\pm$ 38 (614–801)	752 $\pm$ 43 (692–826)	838 $\pm$ 48 (72–913)	892 $\pm$ 66 (777–1009)	745 $\pm$ 160 (508–916)	800 $\pm$ 76 (669–876)
Max. body diameter	44 $\pm$ 2 (38–48)	42 $\pm$ 7 (35–46)	<b>41 <math>\pm</math> 3 (34–46)</b>	49 $\pm$ 2 (43–53)	37 $\pm$ 3 (32–42)	47 $\pm$ 2.2 (43–50)	42 $\pm$ 3 (38–47)	41 $\pm$ 2.3 (36–43)	49 $\pm$ 3.3 (43–55)	49 $\pm$ 4.5 (40–58)	42 $\pm$ 3.9 (34–48)	36 $\pm$ 3 (33–40)
Excretory pore (EP)	95 $\pm$ 12 (78–120)	123 $\pm$ 7 (109–138)	<b>86 <math>\pm</math> 7 (75–102)</b>	81 $\pm$ 7 (71–93)	73 $\pm$ 5 (60–84)	117 $\pm$ 6 (104–128)	124 $\pm$ 10 (108–145)	109 $\pm$ 6 (96–116)	120 $\pm$ 12 (101–145)	135 $\pm$ 11 (104–147)	125 $\pm$ 11.2 (93–141)	89 $\pm$ 2 (86–91)
Nerve ring (NR)	65 $\pm$ 12 (54–88)	75 $\pm$ 4 (72–85)	<b>67 <math>\pm</math> 3 (64–75)</b>	65 $\pm$ 7 (54–77)	71 $\pm$ 5 (60–80)	80 $\pm$ 5 (73–90)	71 $\pm$ 6 (61–83)	79 $\pm$ 5 (71–88)	82 $\pm$ 6 (72–93)	64 $\pm$ 8 (52–81)	69 $\pm$ 11 (54–87)	70 $\pm$ 7 (62–78)
Oesophagus (ES)	112 $\pm$ 13 (85–123)	101 $\pm$ 4 (93–109)	<b>95 <math>\pm</math> 5 (88–106)</b>	116 $\pm$ 10 (105–132)	93 $\pm$ 7 (80–100)	105 $\pm$ 4 (97–111)	96 $\pm$ 5 (89–108)	105 $\pm$ 5 (97–114)	109 $\pm$ 6 (100–122)	115 $\pm$ 5 (105–126)	103 $\pm$ 9 (78–115)	101 $\pm$ 3 (97–106)
Tail length (T)	25 $\pm$ 5 (20–29)	28 $\pm$ 2 (24–32)	<b>25 <math>\pm</math> 2 (21–32)</b>	33 $\pm$ 3 (28–38)	34 $\pm$ 5 (25–45)	34 $\pm$ 6 (29–40)	27 $\pm$ 4 (21–36)	33 $\pm$ 3 (29–41)	33 $\pm$ 4 (29–41)	35 $\pm$ 5 (27–49)	28 $\pm$ 5 (28–46)	32 $\pm$ 2 (29–34)
Anal body diam. (ABD)	25 $\pm$ 3 (21–30)	23 $\pm$ 8 (19–24)	<b>19 <math>\pm</math> 2 (15–22)</b>	22 $\pm$ 1 (20–24)	25 $\pm$ 2 (20–30)	26 $\pm$ 3 (20–31)	24 $\pm$ 1 (23–27)	27 $\pm$ 3 (23–33)	26 $\pm$ 2 (23–28)	24 $\pm$ 3 (18–27)	24 $\pm$ 2 (15–27)	24 $\pm$ 2 (21–28)
Spicule length (SP)	39 $\pm$ 5 (30–42)	43 $\pm$ 3 (35–48)	<b>43 <math>\pm</math> 4 (37–49)</b>	40 $\pm$ 3 (33–45)	39 $\pm$ 3 (31–45)	42 $\pm$ 4 (36–46)	41 $\pm$ 4 (30–47)	41 $\pm$ 3 (35–45)	44 $\pm$ 2 (41–49)	45 $\pm$ 4 (35–54)	43 $\pm$ 4 (34–48)	43 $\pm$ 2 (41–47)
Gubernaculum length (GU)	18 $\pm$ 3 (14–21)	21 $\pm$ 3 (18–23)	<b>20 <math>\pm</math> 2 (17–24)</b>	20 $\pm$ 1.5 (18–22)	22 $\pm$ 3 (20–31)	23 $\pm$ 4 (17–30)	23 $\pm$ 3 (18–32)	21 $\pm$ 2 (19–23)	25 $\pm$ 3 (20–28)	24 $\pm$ 2 (19–27)	22 $\pm$ 3 (16–27)	18 $\pm$ 1 (17–20)
D% = EP/ES $\times$ 100	88 –	121 –	<b>90 <math>\pm</math> 6 (81–108)</b>	70 –	79 $\pm$ 6 (72–91)	112 $\pm$ 4 (105–119)	129 $\pm$ 9 (114–149)	103 $\pm$ 4 (95–109)	110 $\pm$ 6 (100–122)	117 $\pm$ 10 (92–133)	121 $\pm$ 19 (100–172)	– –
SW% = SP/ABD $\times$ 100	156 –	187 –	<b>231 <math>\pm</math> 24 (202–301)</b>	182 $\pm$ 18 (138–208)	150 –	157 $\pm$ 25 (133–209)	167 $\pm$ 20 (130–196)	152 $\pm$ 20 (120–187)	172 $\pm$ 14 (150–200)	196 $\pm$ 32 (130–259)	183 $\pm$ 28 (138–274)	180 $\pm$ 20 (170–220)
GS% = GU/SP $\times$ 100	46 –	50 $\pm$ 10 (40–60)	<b>47 <math>\pm</math> 4 (38–56)</b>	50 $\pm$ 5 (44–61)	60 –	54 $\pm$ 6 (47–65)	56 $\pm$ 7 (43–70)	51 $\pm$ 3 (44–56)	56 $\pm$ 6 (51–64)	54 $\pm$ 5 (43–62)	51 $\pm$ 8 (40–69)	43 $\pm$ 4 (36–47)

EP, distance from anterior end to excretory pore; NR, distance from anterior end to nerve ring; ES, distance from anterior end to end of oesophagus; TAY, *H. taysearae*; IND, *H. indica*; NOE, *H. noenieputensis* n. sp.; BAU, *H. baujardi*; SOR, *H. sonorensis*; FLO, *H. floridensis*; MEX, *H. mexicana*; AMA, *H. amazonensis*; GEO, *H. georgiana*; SAF, *H. safricana*; GER, *H. gerrardi*; DOW, *H. downesi*.

<sup>a</sup> Caborca strain.

<sup>b</sup> Iris strain.

Table 5. Comparative morphometrics of infective juveniles of *Heterorhabditis noenieputensis* n. sp. (in bold) and other related species in order of the length of the infective juvenile. All measurements in  $\mu\text{m}$  and in the form: mean (range) or mean  $\pm$  SD (range).

Character	TAY	IND	NOE	BAU	SOR <sup>a</sup>	FLO	MEX	AMA	GEO	SAF	GER	DOW <sup>b</sup>
	Shamseldean <i>et al.</i> (1996)	Poinar <i>et al.</i> (1992)	n. sp. <b>SF669</b>	Phan <i>et al.</i> (2003)	Stock <i>et al.</i> (2009)	Nguyen <i>et al.</i> (2006)	Nguyen <i>et al.</i> (2004)	Andaló <i>et al.</i> (2006)	Nguyen <i>et al.</i> (2008)	Malan <i>et al.</i> , 2008	Plichta <i>et al.</i> (2009)	Stock <i>et al.</i> (2002) (Irish group)
<i>n</i>	30	25	<b>25</b>	25	25	25	25	20	20	25	25	20
Body length	418 $\pm$ 38 (332–499)	528 $\pm$ 26 (479–573)	<b>536 <math>\pm</math> 21</b> <b>(484–578)</b>	551 $\pm$ 27 (497–595)	557 $\pm$ 28 (495–570)	562 $\pm$ 24 (554–609)	578 $\pm$ 23 (530–620)	589 $\pm$ 12 (567–612)	598 $\pm$ 27 (547–651)	600 $\pm$ 27 (550–676)	604 $\pm$ 39 (551–683)	(637 $\pm$ 32) (588–692)
a	21 $\pm$ 2 (16–27)	26 $\pm$ 4 (25–27)	<b>24 <math>\pm</math> 1</b> <b>(21–27)</b>	28 $\pm$ 1 (26–30)	23 $\pm$ 1.5 (19–26)	28 $\pm$ 5 (25–32)	26 (23–28)	26 $\pm$ 1 (24–29)	27 $\pm$ 3 (23–34)	29 $\pm$ 2 (24.8–31.8)	13 $\pm$ 3 (23–32)	35 $\pm$ 4 (29–42)
b	3.8 $\pm$ 0.2 (3.4–4.2)	4.5 $\pm$ 0.34 (4.3–4.8)	<b>4.9 <math>\pm</math> 0.2</b> <b>(4.3–5.2)</b>	4.8 $\pm$ 0.2 (4.5–5.1)	4.8 $\pm$ 0.4 (4.4–5.4)	4.3 $\pm$ 2.1 (3.9–4.9)	4.6 (4.2–5.1)	4.9 $\pm$ 0.3 (4.4–5.5)	4.7 $\pm$ 0.3 (4.1–5.3)	4.5 $\pm$ 0.2 (3.9–4.9)	0.21 $\pm$ 0.02 (0.14–0.23)	4.7 $\pm$ 0.3 (4.4–5.3)
c	7.7 $\pm$ 0.7 (6.5–8.7)	5.3 $\pm$ 0.5 (4.5–5.6)	<b>6.2 <math>\pm</math> 0.3</b> <b>(5.5–6.8)</b>	6 $\pm$ 0.3 (6–6.7)	5.5 $\pm$ 1.0 (4.0–6.5)	5.6 $\pm$ 2.4 (5.3–6.6)	5.9 (5.5–6.3)	5.5 $\pm$ 0.2 (5.1–6.1)	6.1 $\pm$ 0.4 (5.5–6.9)	6.4 $\pm$ 0.6 (5.4–7.5)	0.17 $\pm$ 0.03 (0.11–0.21)	9.5 $\pm$ 5 (8.5–10.5)
Max. body diam.	20 $\pm$ 2 (17–23)	20 $\pm$ 6 (19–22)	<b>23 <math>\pm</math> 1</b> <b>(21–25)</b>	20 $\pm$ 2 (18–22)	26 $\pm$ 4 (19–32)	21 $\pm$ 5 (19–23)	23 $\pm$ 1 (20–24)	23 $\pm$ 1 (20–24)	22 $\pm$ 2 (17–26)	21 $\pm$ 1 (19–23)	23 $\pm$ 3 (18–29)	18 $\pm$ 2 (15–22)
Excretory pore (EP)	90 $\pm$ 9 (74–113)	98 $\pm$ 7 (88–107)	<b>97 <math>\pm</math> 3</b> <b>(88–105)</b>	97 $\pm$ 3 (91–103)	99 $\pm$ 5 (97–116)	109 $\pm$ 10 (101–122)	102 $\pm$ 5 (83–109)	107 $\pm$ 6 (89–115)	104 $\pm$ 4 (97–113)	110 $\pm$ 4 (103–122)	98 $\pm$ 6 (92–111)	115 $\pm$ 8 (96–128)
NR	74 $\pm$ 7 (58–87)	82 $\pm$ 4 (72–85)	<b>81 <math>\pm</math> 6</b> <b>(69–96)</b>	81 $\pm$ 3 (75–86)	93 $\pm$ 4 (87–98)	86 $\pm$ 9.2 (68–107)	81 $\pm$ 4 (74–88)	85 $\pm$ 5 (76–93)	85 $\pm$ 5 (74–94)	93 $\pm$ 4.0 (86–101)	93 $\pm$ 18 (81–105)	101 $\pm$ 3 (96–105)
ES	110 $\pm$ 8 (96–130)	117 $\pm$ 3 (109–123)	<b>106 <math>\pm</math> 9</b> <b>(79–115)</b>	115 $\pm$ 3 (107–120)	119 $\pm$ 7 (110–131)	135 $\pm$ 11.6 (123–142)	122 $\pm$ 27 (104–142)	121 $\pm$ 6.6 (107–132)	127 $\pm$ 7 (110–139)	131 $\pm$ 3.7 (125–141)	124 $\pm$ 5 (110–130)	134 $\pm$ 4 (126–141)
Tail length with sheath (T)	55 $\pm$ 7 (44–70)	101 $\pm$ 6 (93–109)	<b>86 <math>\pm</math> 3.4</b> <b>(78–95)</b>	90 $\pm$ 4 (83–97)	105 $\pm$ 7 (91–125)	103 $\pm$ 10 (91–113)	99 $\pm$ 4 (91–106)	107 $\pm$ 5 (98–115)	98 $\pm$ 5 (86–108)	93 $\pm$ 6 (86–108)	102 $\pm$ 14 (76–141)	69 $\pm$ 4 (62–74)
Tail length without sheath	–	–	<b>60 <math>\pm</math> 3</b> <b>(55–66)</b>	–	–	63 $\pm$ 7.9 (48–68)	66 $\pm$ 3 (59–73)	69 $\pm$ 4 (59–74)	61 $\pm$ 5 (51–72)	57 $\pm$ 3 (49–62)	–	–
Anal body diam.	–	–	<b>14 <math>\pm</math> 1.0</b> <b>(12–16)</b>	13 $\pm$ 0.7 (11–14)	16 $\pm$ 2.0 (13–16)	14 $\pm$ 3.7 (12–16)	15 $\pm$ 1.2 (12–17)	14 $\pm$ 1.4 (13–17)	15 $\pm$ 1.5 (13–17)	13 $\pm$ 0.6 (12–14)	15 $\pm$ 2.9 (12–21)	12 $\pm$ 1 (9–14)
D% = EP/ES $\times$ 100	83 $\pm$ 6 (71–96)	84 $\pm$ 5 (79–90)	<b>89 <math>\pm</math> 3</b> <b>(81–95)</b>	84 $\pm$ 3 (78–88)	90 $\pm$ 8.5 (78–110)	81 $\pm$ 8.9 (71–90)	81 $\pm$ 3 (72–86)	88 $\pm$ 2.7 (83–92)	– (70–93)	84 $\pm$ 2.6 (80–90)	80 $\pm$ 0.5 (73–92)	85 $\pm$ 5 (76–98)
E% = EP/T $\times$ 100	180 $\pm$ 27 (110–230)	94 $\pm$ 7 (83–103)	<b>113 <math>\pm</math> 6</b> <b>(99–125)</b>	108 $\pm$ 4 (98–114)	99 $\pm$ 8 (81–111)	105 $\pm$ 10 (95–134)	104 $\pm$ 5 (87–111)	100 $\pm$ 6 (89–109)	107 $\pm$ 8 (95–117)	119 $\pm$ 9 (99–133)	99 $\pm$ 2 (73–138)	170 $\pm$ 10 (160–180)

EP, distance from anterior end to excretory pore; NR, distance from anterior end to nerve ring; ES, distance from anterior end to end of oesophagus; TAY, *H. taysearae*; IND, *H. indica*; NOE, *H. noenieputensis* n. sp.; BAU, *H. baujardi*; SOR, *H. sonorensis*; [ FLO, *H. floridensis*; MEX, *H. mexicana*; AMA, *H. amazonensis*; GEO, *H. georgiana*; SAF, *H. safricana*; GER, *H. gerrardi*; DOW, *H. downesi*.

<sup>a</sup> Caborca strain.

<sup>b</sup> Iris strain.

*Heterorhabditis noenieputensis* n. sp.

n. sp. has a very loose sheath, which can either be attached to the head, folded backwards, or can be well in front of the head, showing the dorsal tooth clearly with the use of a light microscope (fig. 4E, F). The IJ of *H. noenieputensis* n. sp. differs from that of *H. gerrardi* in the length of the oesophagus (106 µm versus 124 µm), in the position of the nerve ring (81 µm versus 93 µm) and in the E% (113 versus 99) (table 5).

The associated symbiotic bacterium of *H. noenieputensis* n. sp. differs from that of *H. indica* and has been described as *Photorhabdus luminescens* subsp. *noenieputensis* (Ferreira *et al.*, 2012), while the bacterium associated with *H. indica* is *P. luminescens* subsp. *akhurstii* (Fischer-Le Saux *et al.*, 1999).

### Acknowledgements

The authors wish to thank Citrus Research International (CRI) and the Technology and Human Resources for Industry Programme (THRIP) for funding, and Elma Carstens and John-Henry Daneel for their collecting of the soil samples.

### References

- Andaló, V., Nguyen, K.B. & Moino, A. (2006) *Heterorhabditis amazonensis* n. sp. (Rhabditida: Heterorhabditidae) from Amazonas, Brazil. *Nematology* **8**, 853–867.
- Bedding, R.A. & Akhurst, R.J. (1975) A simple technique for the detection of insect parasitic rhabditid nematodes in soil. *Nematologica* **21**, 109–110.
- Courtney, W.D., Polley, D. & Miller, V.I. (1955) TAF, an improved fixative in nematode technique. *Plant Disease Reporter* **39**, 570–571.
- Dutky, S.R., Thompson, J.V. & Cantwell, G.E. (1964) A technique for the mass propagation of the DD-136 nematode. *Journal of Insect Pathology* **6**, 417–422.
- Ferreira, T., Van Reenen, C., Pages, S., Tailliez, P., Malan, A.P. & Dicks, L.M.T. (2012) Description of *Photorhabdus luminescens* subsp. *noenieputensis* subsp. nov., a symbiotic bacterium associated with a new *Heterorhabditis* species related to *Heterorhabditis indica*. *International Journal of Systematic and Evolutionary Microbiology*, in press. doi:10.1099/ijls.0.044388-0.
- Fischer-Le Saux, M., Viallard, V., Brunel, B., Normand, P. & Boermare, N.E. (1999) Polyphasic classification of the genus *Photorhabdus* and proposal of new taxa: *P. luminescens* subsp. *luminescens* subsp. nov., *P. luminescens* subsp. *akhurstii* subsp. nov., *P. luminescens* subsp. *laumondii* subsp. nov., *P. temperata* sp. nov., *P. temperata* subsp. *temperara* subsp. nov. and *P. asymbiotica* sp. nov. *International Journal of Systematic Bacteriology* **49**, 1645–1656.
- Hatting, J., Stock, S.P. & Hazir, S. (2009) Diversity and distribution of entomopathogenic nematodes (Steinernematidae, Heterorhabditidae) in South Africa. *Journal of Invertebrate Pathology* **102**, 120–128.
- Jukes, T.H. & Cantor, C.R. (1969) Evolution of protein molecules. pp. 21–132 in Munro, H.N. (Ed.) *Mammalian protein metabolism*. New York, Academic Press.
- Kaya, H.K. & Stock, S.P. (1997) Techniques in insect nematology. pp. 281–324 in Lacey, L.A. (Ed.) *Manual of techniques in insect pathology*. San Diego, Academic Press.
- Malan, A.P., Nguyen, K.B. & Addison, M.F. (2006) Entomopathogenic nematodes (Steinernematidae and Heterorhabditidae) from the southwestern parts of South Africa. *African Plant Protection* **12**, 65–69.
- Malan, A.P., Nguyen, K.B., De Waal, J.Y. & Tiedt, L. (2008) *Heterorhabditis safricana* n. sp. (Rhabditida: Heterorhabditidae), a new entomopathogenic nematode from South Africa. *Nematology* **10**, 381–396.
- Malan, A.P., Knoetze, A.P. & Moore, S.D. (2011) Isolation and identification of entomopathogenic nematodes (Heterorhabditidae and Steinernematidae) in citrus orchards in South Africa and their biocontrol potential against false codling moth. *Journal of Invertebrate Pathology* **108**, 115–125.
- Nguyen, K.B. (2007) Methodology, morphology and identification. pp. 59–119 in Nguyen, K.B. & Hunt, D.J. (Eds) *Entomopathogenic nematodes: Systematics, phylogeny and bacterial symbionts*. Leiden, The Netherlands, Brill.
- Nguyen, K.B., Shapiro-Ilan, D.I., Stuart, R.J., McCoy, C.W., James, R.R. & Adams, B.J. (2004) *Heterorhabditis mexicana* n. sp. (Rhabditida: Heterorhabditidae) from Tamaulipas, Mexico, and morphological studies of the bursa of *Heterorhabditis* spp. *Nematology* **6**, 231–244.
- Nguyen, K.B., Gozel, U., Koppenhofer, H.S. & Adams, B.J. (2006) *Heterorhabditis floridensis* n. sp. (Rhabditida: Heterorhabditidae) from Florida. *Zootaxa* **1177**, 1–19.
- Nguyen, K.B., Shapiro-Ilan, D.I. & Mbata, G.N. (2008) *Heterorhabditis georgiana* n. sp. (Rhabditida: Heterorhabditidae) from Georgia, USA. *Nematology* **10**, 433–448.
- Phan, K.L., Subbotin, S.A., Nguyen, N.C. & Moens, M. (2003) *Heterorhabditis baujardi* sp. n. (Rhabditida: Heterorhabditidae) from Vietnam and morphometric data for *H. indica* populations. *Nematology* **5**, 367–382.
- Plichta, K.L., Joyce, S.A., Clarke, D., Waterfield, N. & Stock, S.P. (2009) *Heterorhabditis gerrardi* n. sp. (Nematoda: Heterorhabditidae): the hidden host of *Photorhabdus asymbiotica* (Enterobacteriaceae:  $\gamma$ -Proteobacteria). *Journal of Helminthology* **83**, 309–320.
- Poinar, G.O., Karunakar, G.K. & David, H. (1992) *Heterorhabditis indicus* n. sp. (Rhabditida, Nematoda) from India: separation of *Heterorhabditis* spp. by infective juveniles. *Fundamental and Applied Nematology* **15**, 467–472.
- Saitou, N. & Nei, M. (1987) The neighbor-joining method: a new method for reconstructing phylogenetic trees. *Molecular Biology and Evolution* **4**, 406–425.
- Seinhorst, J.W. (1959) A rapid method for the transfer of nematodes from fixative to anhydrous glycerin. *Nematologica* **4**, 67–69.
- Shamseldan, M.M., Abou-El-Sooud, A.B., Abd-Elgawad, M.M. & Saleh, M.M. (1996) Identification of a new heterorhabditid species from Egypt, *Heterorhabditis tayserae* n. sp. (Rhabditidae: Heterorhabditidae). *Egypt Journal of Biological Control* **6**, 129–138.
- Shapiro-Ilan, D.I., Gouge, D.H. & Koppenhofer, A.M. (2002) Factors affecting commercial success: Case studies in cotton, turf and citrus. pp. 33–365 in Gaugler, R. (Ed.) *Entomopathogenic nematology*. New York, CABI.
- Stock, S.P., Griffin, C.T. & Burnell, A.M. (2002) Morphological characterisation of three isolates of *Heterorhabditis* Poinar, 1976 from the 'Irish group'

- (Nematoda: Rhabditida: Heterorhabditidae) and additional evidence supporting their recognition as a distinct species, *H. downesi* n. sp. *Systemic Parasitology* **51**, 95–106.
- Stock, S.P., Rivera-Orduño, B. & Flores-Lara, Y.** (2009) *Heterorhabditis sonorensis* n. sp. (Nematoda: Heterorhabditidae), a natural pathogen of the seasonal cicada *Diceroprocta ornea* (Walker) (Homoptera: Cicadidae) in the Sonoran desert. *Journal of Invertebrate Pathology* **100**, 175–184.
- Tamura, K., Peterson, D., Peterson, N., Stecher, G., Nei, N. & Kumar, S.** (2011) MEGA5: Molecular evolutionary genetics analysis using maximum likelihood, evolutionary distance, and maximum parsimony methods. *Molecular Biology and Evolution* **28**, 2731–2739.
- Thompson, J.D., Gibson, T.J., Plewniak, F., Jeanmough, F. & Higgins, D.G.** (1997) The CLUSTAL\_X windows interface: Flexible strategies for multiple sequence alignment aided by quality analysis tools. *Nucleic Acids Research* **25**, 4876–4882.
- Vrain, T.C., Wakarchuck, D.A., Lèvesque, A.C. & Hamilton, R.I.** (1992) Intraspecific rDNA restriction fragment length polymorphism in the *Xiphinema americanum* group. *Fundamental Applied Nematology* **15**, 563–573.